Asian Journal of Chemistry; Vol. 38, No. 2 (2026), 452-462
ASIAN JOURNAL OF CHEMISTRY
https://doi.org/10.14233/ajchem.2026.34898

Design, Synthesis and Molecular Docking Study of New Diaryl Sulphide Phenylenediamine Sulphonamide Hybrids as Antibacterial Agents

B.N. AISHWARYA[1,*], P. SURESH YADAV[2], S. NANJUNDA SWAMY[3], K. VAMSI[4], D.M. MANJUNATH[5], A.M. UTTAM[6], C. SUDHARANI[7], M. SUBHOSH CHANDRA[2] and B.S. PRIYA[1,*]

[1]Department of Studies in Chemistry, University of Mysore, Manasagangotri, Mysore-570006, India
[2]Department of Microbiology, Yogi Vemana University, Kadapa-516005, India
[3]Department of Biotechnology, JSS Science and Technology University, Mysore-570006, India
[4]Indian Institute of Science Education and Research (IISER), Tirupati-517619, India
[5]Department of Plant Sciences, School of Life Sciences, University of Hyderabad, Gachibowli-500046, India
[6]Department of Pharmaceutical Chemistry, Shree Dhanvantary Pharmacy College, Kim, Surat-394110, India
[7]Department of Chemistry, Government Degree College, Panyam, Nandyal-518112, India

*Corresponding authors: E-mail: aishwaryabn12@gmail.com; priyabs_chem@yahoo.com

Received: 15 September 2025 *Accepted*: 10 January 2026 *Published online*: 31 January 2026 AJC-22263

Antimicrobial resistance (AMR) is a growing worldwide threat, exacerbated by the overuse or misuse of antibiotics, particularly in regions like India. To address this, a series of new diaryl sulphide phenylenediamine sulphonamide hybrids (**9a-j**) is we synthesised and evaluated for their antibacterial activity against *Corynebacterium* (Gram-positive) and *Escherichia coli* (Gram-negative). Among these, compound **9i** (4-nitro) showed the most potent antibacterial effects, surpassing streptomycin at all concentrations. Structure-activity relationship (SAR) studies revealed that electron-withdrawing groups, particularly nitro and halogens, enhanced the activity, with *para*-substitution being most effective. Molecular docking studies confirmed that compound **9i** exhibited strong binding to bacterial DNA gyrase, supporting its potential as a broad-spectrum antimicrobial agent. These findings highlight the importance of strategic substitutions in developing effective antibiotics to combat AMR.

Keywords: Antibacterial efficacy, Diaryl sulphide, Amide, Sulphonamide, DNA gyrA.

INTRODUCTION

Antimicrobials, including antibiotics, antivirals, antifungals and antiparasitics, are crucial pharmaceutical agents for the prevention and treatment of infectious diseases. Among these, antibiotics are particularly effective against bacterial infections and have been instrumental in improving survival rates for patients undergoing chemotherapy, surgical interventions and managing chronic infections [1]. In densely populated and developing regions, antibiotics play a vital role in reducing infection-related morbidity and mortality, especially in areas with inadequate sanitation, where food-borne, water-borne and air-borne diseases are common [2]. However, the frequent and sometimes improper use of antibiotics has significantly contributed to the rapid development of antimicrobial resistance (AMR). While AMR is a natural phenomenon, its progression has been significantly fuelled by the overuse and misuse of antibiotics. Epidemiological studies consistently show a direct link between increased antibiotic consumption and the development of resistant microbial strains [3]. Alarmingly, it is predicted that by 2050, AMR could cause up to ten million deaths annually worldwide [4].

India serves as a critical example of this issue, being the world's largest consumer of antibiotics. In 2010, India used approximately 12.9 billion antibiotic units, with systemic antibiotics comprising 77.1% of all antibiotic sales by 2019, reflecting a steady rise in usage [5]. The Indian Council of Medical Research (ICMR) has reported an annual increase of 5-10% in resistance to broad-spectrum antibiotics, with estimates suggesting that one in six individuals may carry resistant pathogens [6]. The increasing resistance affects both Gram-positive and Gram-negative bacteria, creating major

obstacles for existing treatment strategies [7]. To address this crisis, a comprehensive strategy is urgently needed, which includes strengthened antibiotic stewardship, enhanced surveillance systems and continued research into novel antimicrobials and alternative therapies.

Heterocyclic compounds play a central role in this process, as they serve as fundamental structures in numerous natural and synthetic drugs [8]. Their structural versatility and broad biological activity make them essential tools in contemporary drug discovery. Notably, in 2021, nine out of twelve drugs approved by the U.S. FDA featured heterocyclic frameworks as key pharmacophores, highlighting their critical importance in pharmaceutical innovation [9].

Diaryl sulphides are an important class of compounds that appear widely across various domains, including natural products [10-12], organic electronic materials [13], agricultural chemicals [14] and biologically active molecules. In addition to their biological relevance, diaryl sulphides also serve as key intermediates in the synthesis of higher oxidation state sulphur compounds such as sulphoxides and sulphones [15]. Notable pharmaceutical agents featuring diaryl sulphide frameworks include anticancer drugs like axitinib and thymitaq [16], the proton pump inhibitor esomeprazole for gastroesophageal reflux disease [17] and the antidepressant vortioxetine [18]. Due to their versatile structures and wide range of applications, the efficient synthesis of diaryl sulphides remains a key focus of ongoing research efforts.

Sulphonamides, another key class of compounds, are critical in inhibiting bacterial growth by interfering with the synthesis of essential metabolites [19]. These compounds act as competitive inhibitors of dihydropteroate synthase, blocking folic acid production and thereby preventing bacterial replication by disrupting DNA and RNA synthesis. While their use has declined due to the rise of more potent antibiotics and concerns over side effects and resistance, sulphonamides continue to offer value in treating a range of diseases, including viral, fungal and cancerous conditions. Current research efforts are focused on modifying sulphonamide structures to enhance their specificity and therapeutic efficacy [20,21]. Amides also serve as crucial structural elements in many biologically active molecules, contributing to a wide range of pharmacological activities. Amide derivatives exhibit diverse bioactivities, including anti-tuberculosis, analgesic, anti-inflammatory, anticonvulsant, insecticidal, antitumor and antifungal properties [22,23]. This makes them invaluable in medicinal chemistry, with ongoing efforts to optimize their properties for specific therapeutic targets.

DNA gyrase, a type II topoisomerase, plays a vital role in regulating the structural state of DNA, converting it between relaxed and supercoiled forms [24]. It is involved in critical cellular processes such as replication, transcription, recombination, repair and chromosome organisation. Due to its pivotal function in maintaining genomic integrity, DNA gyrase has become a favourable target for the development of new antibacterial agents [25]. By simulating the binding of novel new diaryl sulphide phenylenediamine sulphonamide hybrids to DNA gyrase, researchers aim to predict their binding affinity and understand the nature of their interactions with the enzyme's active site.

EXPERIMENTAL

All chemicals were obtained directly from the reputed chemical vendors and used without further purification. The reaction progress was monitored by thin-layer chromatography (TLC) and final products were purified using column chromatography on silica gel (60-120 mesh). Infrared (IR) spectra were recorded using a Shimadzu-8400 spectrometer. Proton ^{1}H NMR and ^{13}C NMR spectra for both intermediates and final compounds were acquired on a Bruker 400 MHz spectrometer, with $CDCl_3$ or DMSO-d_6 as solvents. Tetramethylsilane (TMS) was used as the internal standard, with chemical shifts δ reported in parts per million (ppm) and coupling constants *J* in hertz (Hz). HR-MS was performed using a Xevo TQD Quadrupole mass spectrometer (XVEO-TQD-QCA583).

Synthesis of 2-(phenylthio)aniline (3): Diphenyl disulphide (**1**, 0.6 mmol) and bromobenzene (**2**, 1.2 mmol) in 1 mL of DMSO were mixed in a round bottom flask followed by the gradual addition of potassium *tert*.-butoxide (1.4 mmol) while stirring at 40-45 ºC for 15 min. After completion of the reaction, the mixture was cooled, poured into water and extracted with ethyl acetate (4 × 10 mL). The organic layers were dried Na_2SO_4, filtered and then the residue was purified by using column chromatography (20% EtOAc:*n*-hexane) to obtain pure 2-(phenylthio)aniline (**3**).

Synthesis of 2-chloro-*N*-(2-(phenylthio)phenyl)acetamide (4): A solution of 2-(phenylthio)aniline (**3**, 12 mmol) in 20 mL of THF was cooled to 0 ºC, after which chloroacetyl chloride (14 mmol) was added dropwise. The mixture was then stirred at room temperature for 1.5 h. Upon completion, the reaction mixture was concentrated and extracted using EtOAc and water. The organic phase was washed sequentially with saturated $NaHCO_3$, brine and anhydrous Na_2SO_4. After the solvent removal, the crude product was purified by column chromatography using 12% EtOAc:*n*-hexane, yielding 2-chloro-*N*-(2-(phenylthio)phenyl)acetamide (**4**) as an off-white crystalline solid.

Synthesis of *tert.*-butyl (4-((2-oxo-2-((2-(phenylthio)-phenyl)amino)ethyl)amino)phenul)carbamate (6): A mixture of compound **4** (2 mmol), *tert*-butyl (4-aminophenyl)-carbamate (**5**, 3 mmol), K_2CO_3 (3 mmol), KI (0.01 mmol) and 30 mL of CH_3CN was heated at 80 ºC for 2 h. After the completion, the mixture was cooled and diluted with water, followed by extraction with EtOAc (3 × 15 mL). The combined organic extracts were washed with water, followed by 20 mL of satd. NH_4Cl to eliminate any residual Boc-protected amine and finally with brine. The organic layer was dried over anhydrous Na_2SO_4 and the solvent was removed under reduced pressure to obtain *tert*-butyl (4-((2-oxo-2-((2-(phenylthio)phenyl)amino)ethyl)amino)phenyl)carbamate (**6**) as product.

Synthesis of 2-((4-aminophenyl)amino)-*N*-(2-(phenylthio)phenyl)acetamide (7): Compound **6** (12 mmol) was mixed with trifluoroacetic acid (24 mmol) in 20 mL of DCM and stirred at room temperature for 2 h. Upon completion, the reaction mixture was concentrated to remove solvents. The resulting crude was dissolved in 5 mL of water and the pH was adjusted to 8-9 using a saturated $NaHCO_3$ solution. The aqueous phase was extracted with DCM (3 × 10 mL) and the

combined organic layers were washed sequentially with saturated $NaHCO_3$ solution, brine and water. The organic extract was then dried over anhydrous Na_2SO_4, concentrated under reduced pressure and purified by column chromatography to afford compound **7** as a pale-yellow solid.

General procedure of synthesis of N-(4-((2-oxo-2-((2-(phenylthio)phenyl)amino)ethyl)amino)phenyl)benzamide (9a-j): To a chilled solution of compound **7** (12 mmol) in 5 mL of DMF, aromatic carboxylic acids (**8a-j**, 12 mmol), hydroxybenzotriazole (HOBt, 15 mmol) and (3-dimethylaminopropyl)-ethylcarbodiimide hydrochloride (EDC·HCl, 20 mmol) were added, along with a few drops of N,N-diisopropylethylamine (DIPEA). The reaction mixture was stirred at room temperature for 1 h. After completion, the mixture was poured over crushed ice to induce precipitation (**Scheme-I**). The solid formed was collected by filtration, dried and recrystallised from EtOH to obtain the final products **9a-j**.

4-Chloro-*N*-(4-((2-oxo-2-((2-(phenylthio)phenyl)amino)-ethyl)amino)phenyl)benzamide (9a): Off white solid, yield: 69%; m.p.: 164-166 ºC, m.f.: $C_{27}H_{22}ClN_3O_2S$; IR (KBr, ν_{max}, cm^{-1}): 3264, 2984, 1692, 1534, 1314, 1264, 1232, 1154; ^1H NMR (400 MHz, $CDCl_3$, δ ppm): 9.53 (s, 1H), 9.13 (s, 1H), 7.90-7.84 (m, 2H), 7.67-7.61 (m, 2H), 7.60-7.49 (m, 3H), 7.40-7.29 (m, 5H), 7.26-7.15 (m, 2H), 7.10 (td, *J* = 7.2, 1.3 Hz, 1H), 6.79-6.73 (m, 2H), 6.24 (t, *J* = 5.7 Hz, 1H), 4.01 (d, *J* = 5.7 Hz, 2H); ^{13}C NMR (400 MHz, $CDCl_3$, δ ppm): 168.97, 165.94, 141.76, 140.86, 136.95, 135.67, 134.17, 133.38, 131.04, 130.21, 129.36, 129.08, 129.07, 128.79, 127.70, 124.55, 123.05,

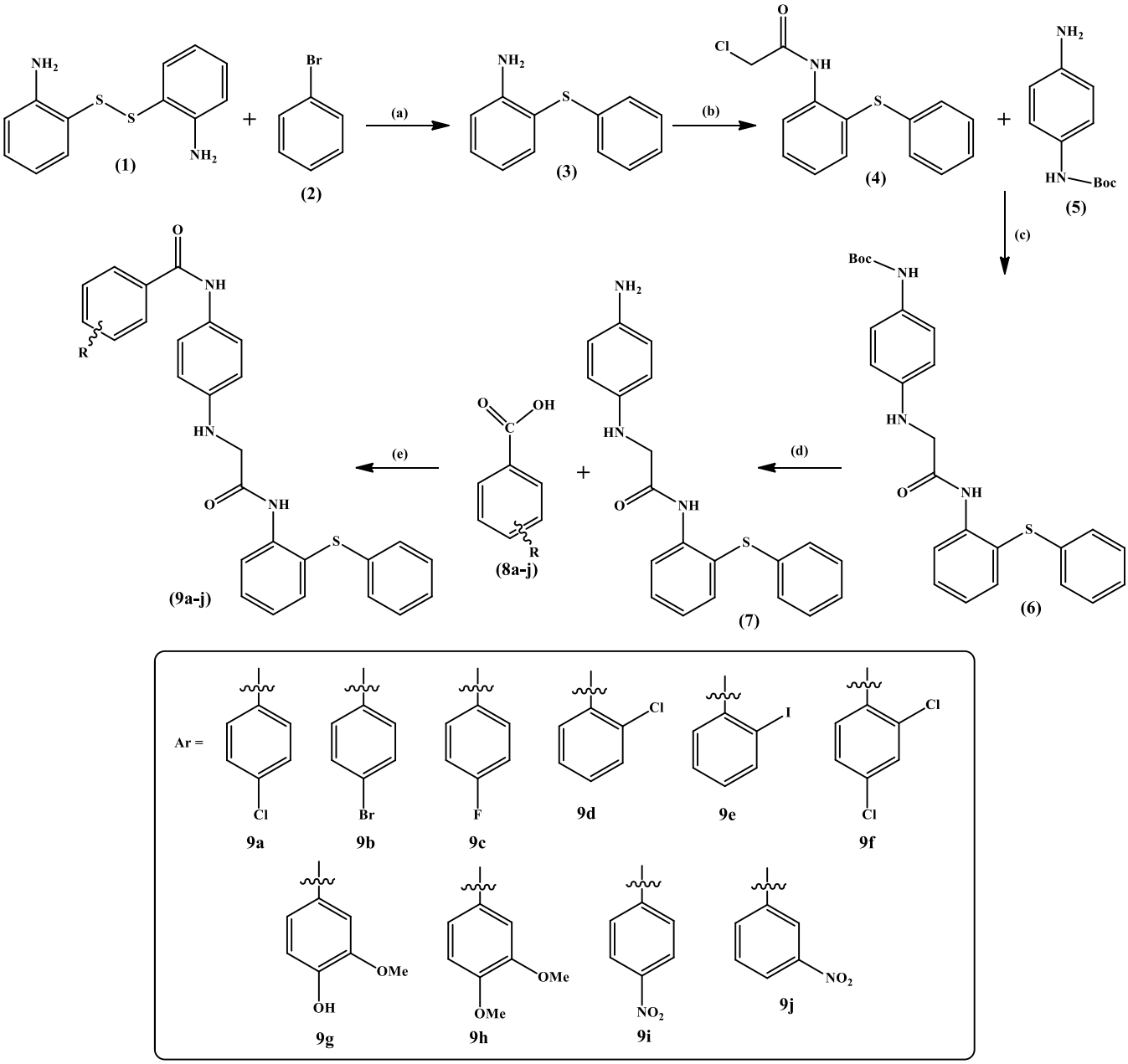

Scheme-I: Synthesis of new diaryl sulphide phenylenediamine sulphonamide derivatives (**9a-j**); Reagents & Conditions: (a) KO*t*Bu, DMSO, 80 ºC; (b) chloroacetylchloride, TEA, THF; (c) K_2CO_3, KI, CH_3CN; (d) TFA, DCM, 2 h; (e) EDC·HCl, HOBt, DIPEA, DMF

122.77, 120.99, 116.34, 45.60; HRMS calcd.: 488.00; found: 489.3234 $[M+H]^+$.

4-Bromo-*N*-(4-((2-oxo-2-((2-(phenylthio)phenyl)amino)-ethyl)amino)phenyl)benzamide (9b): White solid, yield: 74%; m.p.: 169-172 ºC, m.f.: $C_{27}H_{22}BrN_3O_2S$; IR (KBr, ν_{max}, cm^{-1}): 3251, 2963, 1699, 1536, 1333, 1268, 1213, 1152; ^1H NMR (400 MHz, $CDCl_3$, δ ppm): 9.53 (s, 1H), 9.13 (s, 1H), 7.88-7.82 (m, 2H), 7.73-7.67 (m, 2H), 7.67-7.61 (m, 2H), 7.57 (dd, *J* = 7.5, 1.5 Hz, 1H), 7.40-7.29 (m, 5H), 7.26-7.15 (m, 2H), 7.10 (td, *J* = 7.2, 1.3 Hz, 1H), 6.79-6.73 (m, 2H), 6.24 (t, *J* = 5.7 Hz, 1H), 4.01 (d, *J* = 5.7 Hz, 2H); ^{13}C NMR (400 MHz, $CDCl_3$, δ ppm): 168.97, 165.94, 141.76, 140.86, 135.67, 134.17, 133.34, 131.84, 131.04, 130.28, 129.36, 129.08, 128.79, 127.70, 125.42, 124.55, 123.05, 122.77, 120.99, 116.34, 45.60; HRMS calcd. 532.46; found: 533.3486 $[M+H]^+$.

4-Fluoro-*N*-(4-((2-oxo-2-((2-(phenylthio)phenyl)amino)-ethyl)amino)phenyl)benzamide (9c): White solid, yield: 68%; m.p.: 172-176 ºC, m.f.: $C_{27}H_{22}FN_3O_2S$; IR (KBr, ν_{max}, cm^{-1}): 3236, 2984, 1695, 1544, 1329, 1264, 1232, 1152; ^1H NMR (400 MHz, $CDCl_3$, δ ppm): 9.53 (s, 1H), 9.20 (s, 1H), 8.11-8.04 (m, 2H), 7.67-7.61 (m, 2H), 7.57 (dd, *J* = 7.5, 1.4 Hz, 1H), 7.40-7.29 (m, 7H), 7.26-7.15 (m, 2H), 7.13-7.06 (m, 1H), 6.79-6.73 (m, 2H), 6.24 (t, *J* = 5.7 Hz, 1H), 4.01 (d, *J* = 5.7 Hz, 2H); ^{13}C NMR (400 MHz, $CDCl_3$, δ ppm): 168.97, 165.92, 164.82, 163.95, 141.76, 140.86, 135.67, 134.17, 131.13, 131.10, 131.04, 129.88, 129.81, 129.36, 129.08, 128.79, 127.70, 124.55, 123.05, 122.77, 120.99, 116.34, 116.14, 115.96, 45.60; HRMS: calcd.: 471.55; found: 472.6812 $[M+H]^+$.

2-Chloro-*N*-(4-((2-oxo-2-((2-(phenylthio)phenyl)amino)-ethyl)amino)phenyl)benzamide (9d): Brick red solid, yield: 76%; m.p.: 176-180 ºC, m.f.: $C_{27}H_{22}ClN_3O_2S$; IR (KBr, ν_{max}, cm^{-1}): 3232, 2962, 1690, 1532, 1312, 1268, 1218, 1154; ^1H NMR (400 MHz, $CDCl_3$, δ ppm): 9.53 (s, 1H), 8.59 (s, 1H), 7.82 (dd, *J* = 8.0, 1.6 Hz, 1H), 7.67-7.61 (m, 2H), 7.57 (dd, *J* = 7.5, 1.5 Hz, 1H), 7.49 (dd, *J* = 8.0, 1.4 Hz, 1H), 7.45-7.29 (m, 6H), 7.26-7.15 (m, 2H), 7.10 (td, *J* = 7.2, 1.3 Hz, 1H), 6.79-6.66 (m, 3H), 6.24 (t, *J* = 5.7 Hz, 1H), 4.01 (d, *J* = 5.7 Hz, 2H); ^{13}C NMR (400 MHz, $CDCl_3$, δ ppm): 168.97, 165.85, 141.76, 140.86, 135.67, 134.17, 133.52, 133.46, 133.03, 131.56, 129.97, 129.94, 129.36, 129.08, 128.79, 127.70, 127.31, 124.55, 123.05, 122.85, 120.99, 116.37, 45.60; HRMS: calcd. 488.00; found: 489.2135 $[M+H]^+$.

2-Iodo-*N*-(4-((2-oxo-2-((2-(phenylthio)phenyl)amino)-ethyl)amino)phenyl)benzamide (9e): Off white solid, yield: 69%; m.p.: 164-166 ºC, m.f.: $C_{27}H_{22}IN_3O_2S$; IR (KBr, ν_{max}, cm^{-1}): 3252, 2990, 1692, 1524, 1333, 1264, 1212, 1153; ^1H NMR (400 MHz, $CDCl_3$, δ ppm): 9.53 (s, 1H), 8.47 (s, 1H), 7.88 (dd, *J* = 7.5, 1.4 Hz, 1H), 7.81 (dd, *J* = 7.7, 1.5 Hz, 1H), 7.67-7.61 (m, 2H), 7.57 (dd, *J* = 7.5, 1.5 Hz, 1H), 7.45-7.27 (m, 7H), 7.27-7.15 (m, 2H), 7.10 (td, *J* = 7.2, 1.3 Hz, 1H), 6.79-6.73 (m, 2H), 6.24 (t, *J* = 5.7 Hz, 1H), 4.01 (d, *J* = 5.7 Hz, 2H); ^{13}C NMR (400 MHz, $CDCl_3$, δ ppm): 169.65, 167.11, 142.23, 140.27, 140.16, 140.10, 135.67, 134.87, 134.40, 130.06, 129.36, 129.08, 128.99, 128.41, 128.38, 127.70, 124.55, 122.37, 121.98, 121.05, 116.15, 94.28, 45.30; HRMS: calcd. 579.46; found: 580.3215 $[M+H]^+$.

2,4-Dichloro-*N*-(4-((2-oxo-2-((2-(phenylthio)phenyl)-amino)ethyl)amino)phenyl)benzamide (9f): Pale pink solid, yield: 72%; m.p.: 168-174 ºC, m.f.: $C_{27}H_{21}Cl_2N_3O_2S$; IR (KBr, ν_{max}, cm^{-1}): 3222, 2972, 1686, 1522, 1342, 1268, 1244, 1156; ^1H NMR (400 MHz, $CDCl_3$, δ ppm): 9.53 (s, 1H), 8.43 (s, 1H), 7.83-7.74 (m, 2H), 7.67-7.61 (m, 2H), 7.60-7.52 (m, 2H), 7.40-7.29 (m, 5H), 7.26-7.15 (m, 2H), 7.10 (td, *J* = 7.2, 1.3 Hz, 1H), 6.79-6.73 (m, 2H), 6.24 (t, *J* = 5.7 Hz, 1H), 4.01 (d, *J* = 5.7 Hz, 2H); ^{13}C NMR (400 MHz, $CDCl_3$, δ ppm): 168.97, 165.51, 141.76, 140.86, 136.83, 135.67, 134.17, 134.01, 133.97, 131.86, 130.56, 130.01, 129.36, 129.08, 128.79, 127.70, 127.50, 124.55, 123.05, 122.85, 120.99, 116.37, 45.60; HRMS calcd.: 522.44; found: 580.3215 $[M+H]^+$.

4-Hydroxy-3-methoxy-*N*-(4-((2-oxo-2-((2-(phenylthio)-phenyl)amino)ethyl)amino)phenyl)benzamide (9g): Off white solid, yield: 79%; m.p.: 180-183 ºC, m.f.: $C_{28}H_{25}N_3O4S$; IR (KBr, ν_{max}, cm^{-1}): 3230, 2998, 1694, 1542, 1322, 1267, 1232, 1158; ^1H NMR (400 MHz, $CDCl_3$, δ ppm): 9.53 (s, 1H), 8.55 (s, 1H), 7.67-7.61 (m, 3H), 7.57 (dd, *J* = 7.5, 1.4 Hz, 1H), 7.51 (dd, *J* = 8.9, 2.1 Hz, 1H), 7.40-7.29 (m, 6H), 7.26-7.15 (m, 2H), 7.13-7.06 (m, 1H), 6.92 (d, *J* = 8.9 Hz, 1H), 6.79-6.73 (m, 2H), 6.24 (t, *J* = 5.7 Hz, 1H), 4.01 (d, *J* = 5.7 Hz, 2H), 3.86 (s, 3H); ^{13}C NMR (400 MHz, $CDCl_3$, δ ppm): 168.97, 166.16, 148.18, 147.40, 141.76, 140.86, 135.67, 134.17, 131.17, 129.36, 129.08, 128.79, 127.70, 125.54, 124.55, 123.41, 123.05, 122.88, 120.99, 116.35, 114.25, 111.47, 56.09, 45.60; HRMS calcd.: 499.59; found: 500.6412 $[M+H]^+$.

3,4-Dimethoxy-*N*-(4-((2-oxo-2-((2-(phenylthio)phenyl)-amino)ethyl)amino)phenyl)benzamide (9h): White solid, yield: 76%; m.p.: 178-182 ºC, m.f.: $C_{29}H_{27}N_3O_4S$; IR (KBr, ν_{max}, cm^{-1}): 3226, 2989, 1699, 1534, 1335, 1269, 1218, 1158; ^1H NMR (400 MHz, $CDCl_3$, δ ppm): 9.53 (s, 1H), 8.55 (s, 1H), 7.67-7.61 (m, 2H), 7.57 (dd, *J* = 7.5, 1.4 Hz, 1H), 7.50 (dd, *J* = 8.4, 2.0 Hz, 1H), 7.40-7.29 (m, 5H), 7.26-7.15 (m, 2H), 7.13-7.06 (m, 1H), 6.97 (d, *J* = 8.4 Hz, 1H), 6.79-6.73 (m, 2H), 6.24 (t, *J* = 5.7 Hz, 1H), 4.01 (d, *J* = 5.8 Hz, 2H), 3.86 (d, *J* = 9.2 Hz, 6H); ^{13}C NMR (400 MHz, $CDCl_3$, δ ppm): 168.97, 166.19, 152.96, 149.25, 141.76, 140.86, 135.67, 134.17, 131.17, 129.36, 129.29, 129.08, 128.79, 127.70, 126.68, 124.55, 123.05, 122.88, 120.99, 116.35, 112.25, 111.41, 55.98, 55.94, 45.60; HRMS: calcd.: 513.61; found: 514.1142 $[M+H]^+$.

4-Nitro-*N*-(4-((2-oxo-2-((2-(phenylthio)phenyl)amino)-ethyl)amino)phenyl)benzamide (9i): Yellow solid, yield: 72%; m.p.: 183-185 ºC, m.f.: $C_{27}H_{22}N_4O_4S$; IR (KBr, ν_{max}, cm^{-1}): 3266, 2989, 1689, 1529, 1329, 1268, 1219, 1152; ^1H NMR (400 MHz, $CDCl_3$, δ ppm): 9.53 (s, 1H), 9.10 (s, 1H), 8.40-8.34 (m, 2H), 8.26-8.20 (m, 2H), 7.67-7.61 (m, 2H), 7.57 (dd, *J* = 7.5, 1.5 Hz, 1H), 7.40-7.29 (m, 5H), 7.26-7.15 (m, 2H), 7.10 (td, *J* = 7.2, 1.3 Hz, 1H), 6.79-6.73 (m, 2H), 6.24 (t, *J* = 5.7 Hz, 1H), 4.01 (d, *J* = 5.7 Hz, 2H); ^{13}C NMR (400 MHz, $CDCl_3$, δ ppm): 168.97, 164.62, 148.75, 141.76, 140.86, 140.35, 135.67, 134.17, 131.04, 129.58, 129.36, 129.08, 128.79, 127.70, 124.55, 123.70, 123.05, 122.77, 120.99, 116.34, 45.60; HRMS: calcd.: 498.56; found: 499.4263 $[M+H]^+$.

3-Nitro-*N*-(4-((2-oxo-2-((2-(phenylthio)phenyl)amino)-ethyl)amino)phenyl)benzamide (9j): Pale yellow solid, yield: 73%; m.p.: 178-182 ºC, m.f.: $C_{27}H_{22}N_4O_4S$; IR (KBr, ν_{max}, cm^{-1}): 3246, 2982, 1692, 1532, 1312, 1264, 1232, 1154; ^1H NMR (400 MHz, $CDCl_3$, δ ppm): 9.53 (s, 1H), 8.87 (t, *J* = 2.1 Hz, 1H), 8.58 (s, 1H), 8.43 (ddd, *J* = 9.0, 2.2, 1.3 Hz, 1H),

8.30 (ddd, *J* = 8.0, 2.2, 1.2 Hz, 1H), 7.83 (dd, *J* = 8.9, 8.2 Hz, 1H), 7.67-7.61 (m, 2H), 7.57 (dd, *J* = 7.5, 1.5 Hz, 1H), 7.40-7.29 (m, 5H), 7.26-7.15 (m, 2H), 7.10 (td, *J* = 7.2, 1.3 Hz, 1H), 6.79-6.73 (m, 2H), 6.24 (t, *J* = 5.7 Hz, 1H), 4.01 (d, *J* = 5.7 Hz, 2H); ^{13}C NMR (400 MHz, $CDCl_3$, δ ppm): 168.97, 166.40, 147.81, 141.76, 140.86, 135.67, 134.17, 133.96, 133.21, 131.34, 130.43, 129.36, 129.08, 128.79, 127.70, 125.97, 124.55, 123.66, 123.05, 122.88, 120.99, 116.35, 45.60; HRMS: calcd.: 498.56; found: 499.2132 $[M+H]^+$.

Antibacterial activity: Agarose gel electrophoresis was carried out using gels prepared with 4% Tris-Borate-EDTA (TBE) buffer. Fluorescence signals were visualised and quantified using a double fluorescence FMYG100 microscope. For cytofluorometric analysis, a Beckman Coulter Gallios 10/3 flow cytometer was employed. The *in vitro* antibacterial efficacy of the newly synthesised diaryl sulphide phenylenediamine sulphonamide hybrids (**9a-j**) was assessed using the agar well diffusion technique on Mueller-Hinton Agar (MHA). Both Gram-positive *Corynebacterium* and Gram-negative *Escherichia coli* bacterial strains were tested at concentrations of 25, 50, 75 and 100 μg/mL. Standard antibiotic streptomycin was used as references at 100 μg/mL. Nutrient agar and agar plates from Merck were employed to generate a bacterial load ranging between 10^4 and 10^6 colony-forming units (CFU). A sterile cork borer was used to punch aseptic wells measuring 6-8 mm in diameter, spaced 25 mm apart. Each well was loaded with 10 μL of the test compounds dissolved in DMSO and the plates were incubated at 37 ºC for 24 h. The appearance of clear zones around the wells signified antibacterial action and the diameter of these inhibition zones correlated with the extent of bacterial growth suppression. The agar dilution method was employed to determine the diameter of inhibition zones (DIZ), indicating the lowest concentration at which bacterial growth was prevented.

Molecular docking: A molecular docking study was carried out to explore the antibacterial mode of action and the intermolecular interactions of small-molecule compounds. Molecular docking simulations were performed using the Molecular Operating Environment (MOE) software suite, version 2015, with DNA gyrase A from *Escherichia coli* as the target protein. The crystal structure of the protein was obtained from the Protein Data Bank (PDB), while the chemical structures of the compounds were created using ChemDraw. Protein preparation involved using the structure preparation wizard, which included adding hydrogen atoms, removing water molecules and carrying out energy minimisation to optimize the structure. The prepared protein was then saved for docking. Docking parameters were configured by defining the active site with dummy atoms, using the triangle matcher algorithm for ligand placement, London dG for initial scoring, a rigid receptor model for refinement and GBVI/WSA dG for final scoring and pose selection. The three ligand structures were imported as MDB files and general docking calculations were executed automatically. Upon completion of the docking procedure, the resulting binding poses were analysed to evaluate the interactions between the ligands and the target protein [21,26,27].

RESULTS AND DISCUSSION

The diaryl sulphide phenylenediamine sulphonamide hybrids (**9a-j**) were efficiently synthesised through a concise multi-step sequence. Beginning with diphenyl disulphide and bromobenzene, 2-(phenylthio)aniline (**3**) was obtained *via* a nucleophilic substitution catalysed by KO*t*Bu in DMSO. This intermediate was then selectively acylated with chloroacetyl chloride to yield compound **4**. Building on this, nucleophilic substitution of **4** with *tert*-butyl(4-aminophenyl)carbamate (**5**) afforded compound **6** under mild conditions. Subsequent removal of the Boc protecting group using TFA generated the key intermediate **7**, which served as the scaffold for further derivatisation. By introducing various substituents onto this scaffold, a series of ten DAS derivatives (**9a-j**) were synthesised with moderate to good yields. This synthetic strategy allowed for systematic variation of electronic and steric properties, facilitating comprehensive structure-activity relationship studies. The structures were confirmed through FT-IR, ^{1}H NMR, ^{13}C NMR and HR-MS spectral recordings.

Antibacterial activity: The antibacterial potential of the newly synthesised diaryl sulphide phenylenediamine sulphonamide hybrids (**9a-j**) was systematically evaluated against both *Corynebacterium* (Gram-positive) and *E. coli* (Gram-negative) strains using the minimal inhibition zone (MIZ) assay at four concentrations (25, 50, 75 and 100 μL). Streptomycin served as the standard reference. The data, presented in Table-1,

TABLE-1
MINIMAL INHIBITION ZONES (MIZ, mm) OF ANTIBACTERIAL ACTIVITY OF COMPOUNDS **9a-j** AGAINST TWO BACTERIAL STRAINS AT FOUR DIFFERENT CONCENTRATIONS

Strains	Gram-positive bacterium (*Corynebacterium*)					Gram-negative bacterium (*Escherichia coli*)				
Conc. (μL)	25	50	75	100	Streptomycin	25	50	75	100	Streptomycin
9a	14	15	16	18	21	13	14	17	18	21
9b	18	19	23	23	21	16	18	22	23	21
9c	16	17	19	19	21	16	16	19	20	21
9d	17	18	20	21	21	16	16	20	20	21
9e	10	12	13	15	21	10	11	14	15	21
9f	13	14	15	17	21	12	13	15	16	21
9g	11	14	15	17	21	10	13	14	16	21
9h	18	19	22	23	21	17	18	20	22	21
9i	20	25	26	31	21	21	25	27	30	21
9j	20	23	24	24	21	19	23	25	25	21

revealed a distinct concentration-dependent response, with clear variation in activity based on the nature and position of substituents on the aryl carboxamide framework.

Across the series, compound **9i** (4-nitro) demonstrated exceptional antibacterial activity against *Corynebacterium*, exhibiting MIZ values of 20-31 mm from the lowest to highest concentration. This performance notably surpassed the standard drug, streptomycin (21 mm), at all tested concentrations. The remarkable potency of compound **9i** underscores the critical role of strong electron-withdrawing groups, such as *para*-nitro, in enhancing interaction with bacterial targets. Complementing this, compound **9j** (3-nitro) also displayed robust inhibitory effects, reaching a MIZ of 24 mm at 100 μL. Although slightly less active than its *para*-substituted counterpart, compound **9j** reinforces the importance of nitro substitution for antibacterial efficacy, with subtle positional effects modulating potency. Further analysis revealed that halogen-substituted analogs demonstrated varied activity depending on both the halogen type and its position. For instance, compound **9b** (4-bromo) consistently outperformed both compounds **9a** (4-chloro) and **9c** (4-fluoro), suggesting that bromine's higher polarizability and size may facilitate stronger interactions with microbial enzymes or membranes. Notably, compound **9d** (2-chloro) exhibited greater activity than its *para*-analogue (**9a**), highlighting the potential steric and electronic benefits of *ortho*-substitution. This trend was also reflected in disubstituted analogs. For example, compound **9f** (2,4-dichloro) demonstrated moderate activity (up to 17 mm), while methoxy-bearing derivatives, particularly compound **9h** (3,4-dimethoxy), showed enhanced potency (up to 23 mm), suggesting that electron-donating groups, when properly oriented, can also support antibacterial action. In contrast, compound **9e** (2-iodo) exhibited the lowest activity (maximum 15 mm), likely due to steric hindrance and reduced electronic contribution from the bulky iodine atom.

A similar activity pattern was observed against the Gram-negative strain *E. coli*, although slight differences in magnitude were observed. Compound **9i** once again emerged as the most potent derivative, achieving a peak inhibition zone of 30 mm at 100 μL, significantly exceeding the standard. This consistent, dual-strain efficacy underscores the broad-spectrum potential of 4-nitro substitution. Likewise, compound **9j** maintained strong activity, reaching 25 mm, while compounds **9b** (4-bromo) and **9h** (3,4-dimethoxy) followed closely behind, with MIZ values of 23 mm and 22 mm, respectively. These results affirm that both electron-withdrawing and moderately electron-donating substituents, when appropriately positioned, contribute positively to antibacterial performance. Interestingly, fluorinated (**9c**) and chlorinated (**9a**) analogs displayed moderate efficacy, while compound **9e** (2-iodo) again showed the lowest activity, indicating a clear trend were substituent size and electronic properties impact membrane penetration and bacterial enzyme inhibition. The disubstituted analog **9f** performed comparably against both bacterial strains, though less effectively than mono-nitro or bromo compounds. Taken together, the antibacterial data suggest that compounds **9i**, **9j** and **9b** consistently outperformed streptomycin, particularly at higher concentrations. Notably, their superior inhibition against both Gram-positive and Gram-negative bacteria highlights their potential as broad-spectrum antibacterial agents. Methoxy-bearing analogs such as **9h** also showed promising dual-strain activity, making them worthy candidates for further optimisation.

A comprehensive SAR analysis reveals that electron-withdrawing groups, especially nitro (NO_2) and halogens (Cl, Br), significantly enhance antibacterial activity, particularly when positioned at the *para* or *ortho* positions. The 4-nitro (**9i**) and 3-nitro (**9j**) analogs emerged as the most potent, underscoring the importance of both electronic effects and substituent orientation. Furthermore, *ortho*-substituted halogens (*e.g.*, 2-chloro in **9d**) generally showed higher activity than their *para*-analogs, suggesting spatial advantages in binding. Disubstitution (*e.g.*, 3,4-dimethoxy in **9h**) also contributed to improved potency, likely due to synergistic electronic interactions. Conversely, bulky or less electronegative groups, such as iodine (**9e**), were associated with diminished activity, likely due to steric hindrance and suboptimal molecular interactions.

Molecular docking: To gain a deeper understanding of the antibacterial efficacy observed in the diaryl sulphide phenylenediamine sulphonamide hybrids (**9a-j**), molecular docking studies were conducted, targeting the bacterial active site and the results were systematically correlated with the structure-activity relationship (SAR) and minimal inhibition zone (MIZ) data. Docking scores, RMSD values and key binding site interactions provided valuable insights into how the structural modifications influenced biological activity.

Among the entire series, compound **9i** (4-nitro) emerged as the most potent antibacterial agent in the series, exhibiting the highest docking score (-8.31 kcal/mol), stable binding (RMSD: 2.2 Å) and strong interactions with key residues *viz*. Ser97 (3.29 Å), Asn269 (3.09 Å) and Phe96 (3.67 Å). The *para*-nitro group, with its strong electron-withdrawing nature, enhances hydrogen bonding and π-π stacking, contributing to excellent *in vitro* activity against *Corynebacterium* (MIZ: 31 mm) and *Escherichia coli* (MIZ: 30 mm). However, on shifting the nitro group to the *meta* position in compound **9j**, a noticeable reduction in activity was observed (MIZ: 24-25 mm), along with a slightly lower docking score (-7.76 kcal/mol) despite a better RMSD (1.37 Å). It formed interactions with Met120 (3.24 Å) and Ser116 (3.76 Å), but the altered positioning reduced the effectiveness of key binding interactions (Table-2). This clearly indicates that nitro substitution at the *para* position is more favourable for antibacterial activity, establishing a consistent SAR trend across the series.

Halogen-substituted compounds further highlighted the role of electronic effects and substitution patterns in modulating activity. Among them, compound **9b** (4-bromo) demonstrated strong antibacterial performance (MIZ: 23 mm for both strains), a high docking score (-7.74 kcal/mol) and stable binding (RMSD: 1.49 Å). Its interactions with Gln94, Arg91 and Asn269 suggest that bromine's optimal size and polarizability facilitate favourable van der Waals and electrostatic interactions. In contrast, compounds **9a** (4-chloro) and **9c** (4-fluoro) showed reduced activity and slightly lower docking scores (-7.39 kcal/mol and -7.46 kcal/mol, respectively). While both formed interactions **9a** with Ser97, Ala117 and Phe96 and **9c** with Arg91 and Ala117 their smaller size or higher

TABLE-2
MOLECULAR INTERACTION OF COMPOUNDS WITH DNA Gyr.A OF BACTERIA
DOCKING SCORES, rmsd_refine AND MOLECULAR INTERACTION WITH BOND LENGTH

Compound	Docking score (kcal/mol)	rmsd_refine	Residue (distance, Å)
9a	-7.38525	2.34	Ser97 (3.34), Ala117 (3.37), Phe96 (3.71)
9b	-7.74219	1.49	Gln94 (3.06), Arg91 (3.17), Asn269 (3.54)
9c	-7.45747	2.33	Arg91 (2.87), Ala117 (2.98)
9d	-7.62209	2.32	Arg91 (4.22), Asn269 (4.06)
9e	-7.04698	3.17	Asp87 (2.96), Ala117 (2.90), Asn269 (4.83)
9f	-7.37611	2.02	Ser83 (3.97), Asp87 (3.84)
9g	-7.36923	1.61	Asp87 (2.93), Phe96 (3.67), Ser116 (3.66)
9h	-7.71858	2.26	Asp87 (3.00), Arg91 (3.52)
9i	-8.31350	2.20	Ser97 (3.29), Asn269 (3.09), Phe96 (3.67)
9j	-7.75918	1.37	Met120 (3.24), Ser116 (3.76)
Streptomycin	-7.39743	2.17	Ser116 (3.07), Asp87 (3.30), Asp87 (2.92), Arg91 (3.34), Arg91 (3.19), Asp87 (3.50), Asp87 (3.30), Asp87 (2.92), Asp87 (4.00)

electronegativity likely limited binding efficiency. These results indicate that bromo substitution offers a clear advantage over fluoro and chloro analogs in this scaffold. Interestingly, compound **9d** (2-chloro) showed greater antibacterial activity than its *para* isomer **9a**, despite a slightly lower docking score (-7.62 kcal/mol). Its interactions with Arg91 (4.22 Å) and Asn269 (4.06 Å), though weaker in distance, suggest that *ortho*-substitution may allow a better spatial fit within the active site. This trend was further supported by compound **9f** (2,4-dichloro), which showed moderate activity (MIZ: 17 mm) and docking affinity (-7.38 kcal/mol), indicating that disubstitution is tolerated but may not confer additional benefit unless steric and electronic factors are optimally aligned.

Among the electron-donating derivatives, compound **9h** (3,4-dimethoxy) exhibited a respectable docking score (-7.72 kcal/mol) and stable binding (RMSD: 2.26 Å), forming key interactions with Asp87 (3.00 Å) and Arg91 (3.52 Å). These are likely mediated by hydrogen bonding and dipole-dipole interactions facilitated by the methoxy groups. Correspondingly, **9h** demonstrated notable antibacterial activity (MIZ up to 23 mm), suggesting that well-positioned electron-donating groups can enhance biological performance potentially by improving molecular conformation, solubility and cell permeability in addition to target binding. In contrast, compound **9e** (2-iodo) emerged as the least effective antibacterial agent (MIZ: 15 mm), with the lowest docking score (-7.05 kcal/mol) and the highest RMSD (3.17 Å), indicating weak and unstable binding. Although it interacted with Asp87 and Ala117, the longer interaction distances and the bulky iodine atom likely introduced steric hindrance, disrupting optimal fit within the binding pocket. This underscores a key SAR insight: bulky, non-polarizable substituents diminish both binding affinity and biological activity by limiting active site complementarity and reducing favourable interactions.

Other compounds, such as compounds **9g** (4-hydroxy) and **9f** (2,4-dichloro), showed moderate docking scores and antibacterial activity, reinforcing the idea that hydrophilic or moderately electronegative groups can support target binding but only when precisely positioned. For instance, compound **9g** formed interactions with Asp87, Phe96 and Ser116 and had a docking score of -7.37 kcal/mol, which correlates well with its moderate antibacterial activity (MIZ: 17 mm). When compared to the standard antibiotic streptomycin, which had a docking score of -7.40 kcal/mol and interacted with Asp87, Arg91 and Ser116, several synthetic derivatives particularly compounds **9i**, **9j** and **9b** exhibited even stronger binding affinities and superior antibacterial activity. While the multiple interactions of streptomycin suggest a distinct binding mechanism or pharmacophore footprint, the sulphonamide derivatives demonstrate comparable or improved efficiency within the same target site.

Thus, the molecular docking results (Fig. 1) align well with the experimental antibacterial data and strongly support the observed structure activity relationships. Electron-withdrawing groups, especially nitro and bromo at the *para* or *meta* positions, significantly enhance both binding affinity and biological activity. *ortho*-Halogenation, as seen in compound **9d**, appears to offer spatial advantages that improve binding. In contrast, bulky substituents like iodine (as in **9e**) negatively impact both affinity and efficacy due to steric hindrance. The electron-donating groups such as methoxy (**9h**) can also enhance activity when strategically positioned. This integrated analysis clearly demonstrates that substitution patterns on the aryl ring play a critical role in shaping molecular interactions and biological potential, highlighting the promise of these sulphonamide derivatives as broad-spectrum antibacterial agents.

Conclusion

A new series of diaryl sulphide phenylenediamine sulphonamide hybrids (**9a-j**) was successfully synthesised through an efficient multi-step approach and evaluated for their antibacterial potential. Both experimental and computational studies revealed a strong correlation between electronic properties, substitution patterns and biological activity. Among the series, compound **9i** (4-nitro) consistently demonstrated the highest antibacterial efficacy and docking affinity, highlighting the significant role of electron-withdrawing groups in enhancing target interaction. Other potent analogs, including **9j** (3-nitro) and **9b** (4-bromo), further supported this trend. In contrast, compounds bearing bulky or weakly interacting groups, such as **9e** (2-iodo), showed reduced activity due to steric hindrance and poor binding. SAR analysis indicated that *para*- and *ortho*-substitutions, particularly with halogens or nitro

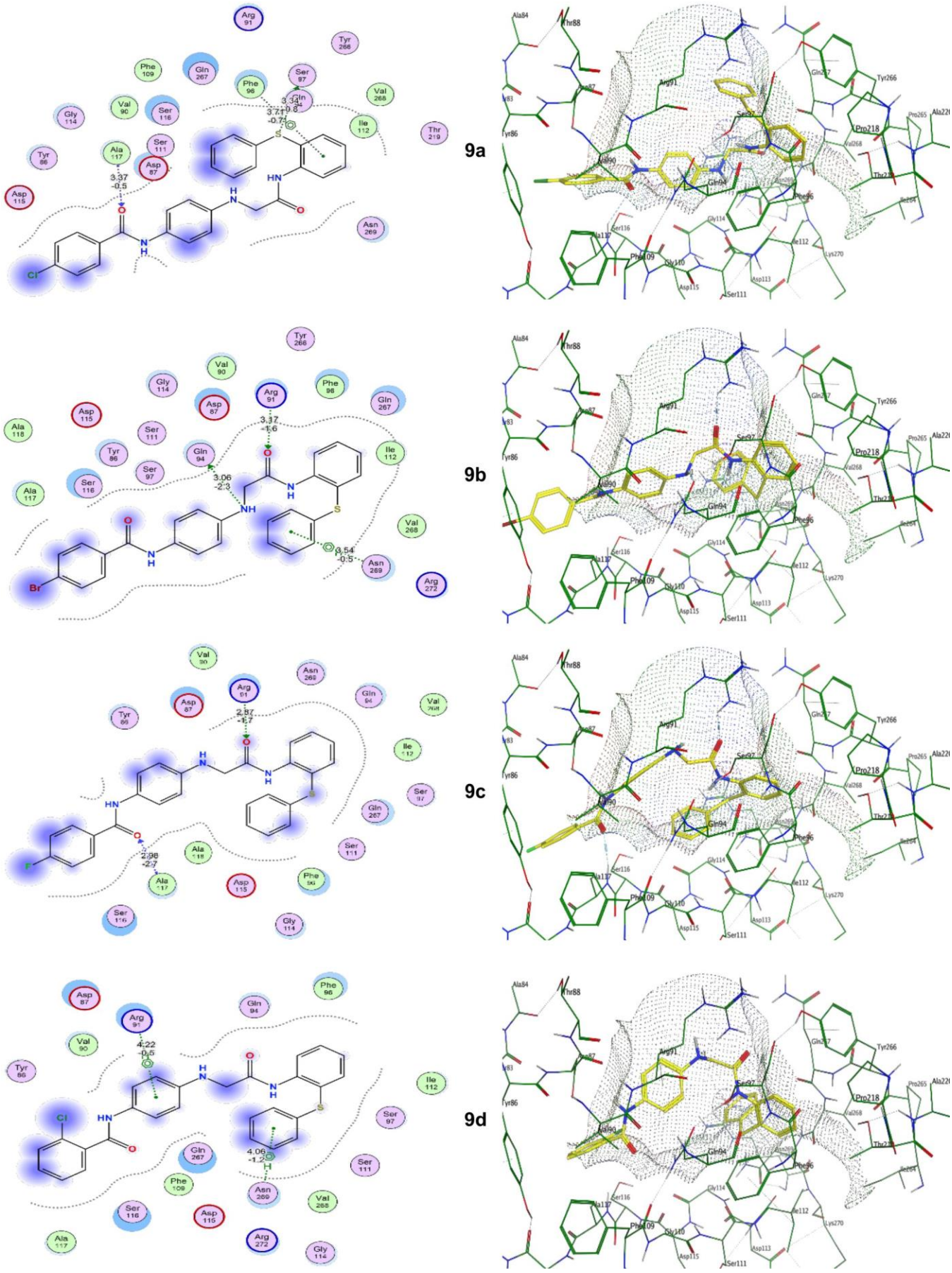
9a
9b
9c
9d

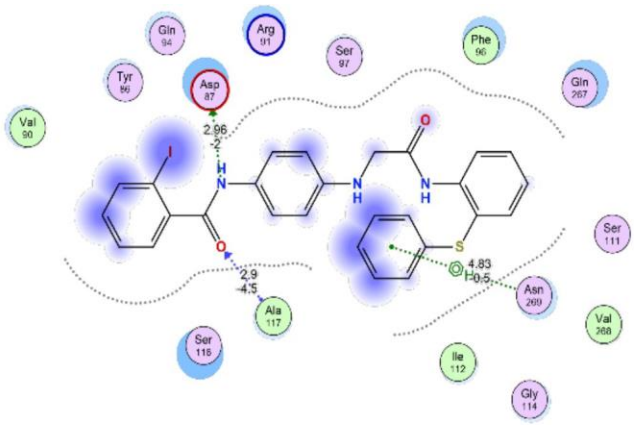
Gln 94
Arg 91
Ser 97
Phe 96
Tyr 86
Asp 87
Gln 267
Val 90
2.96
-2
I
H
N
N
H
N
H
O
O
S
4.83
-0.5
2.9
-4.5
Ser 111
Asn 269
Ala 117
Val 268
Ser 118
Ile 112
Gly 114

9e

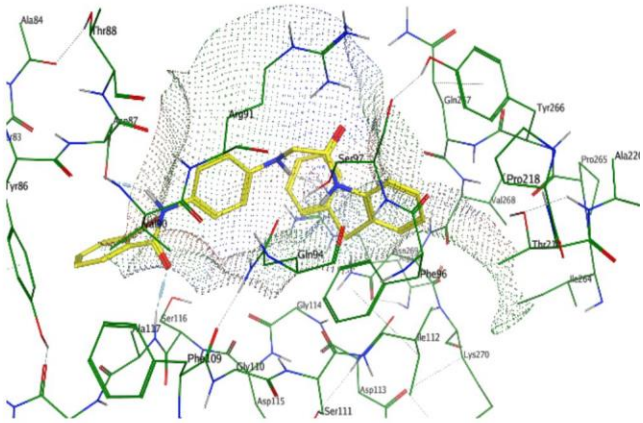
Ala84
Thr88
Arg91
Ser97
Tyr86
Gln267
Tyr266
Pro265
Pro218
Val268
Thr219
Gln94
Phe96
Gly114
Ile112
Lys270
Ser116
Ala117
Phe109
Gly110
Asp113
Asp115
Ser111

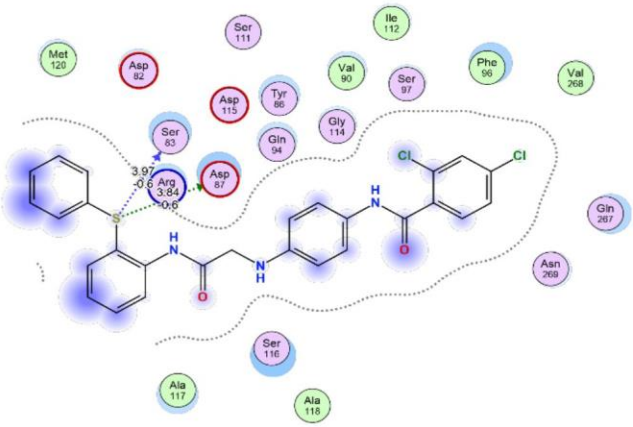
Ile 112
Ser 111
Met 120
Asp 82
Val 90
Phe 96
Ser 97
Val 268
Asp 115
Tyr 86
Gly 114
Ser 83
Gln 94
3.97
-0.6
Arg 91
3.84
-0.6
Asp 87
Cl
Cl
H
N
N
H
N
H
O
O
S
Gln 267
Asn 269
Ser 116
Ala 117
Ala 118

9f

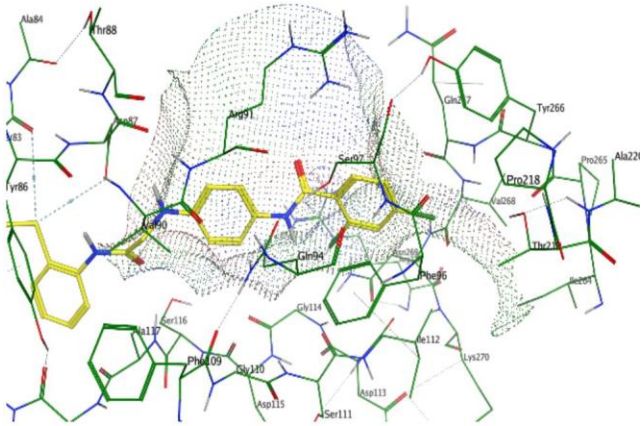
Ala84
Thr88
Arg91
Ser97
Tyr86
Gln267
Tyr266
Pro265
Pro218
Val268
Thr219
Gln94
Phe96
Gly114
Ile112
Lys270
Ser116
Ala117
Phe109
Gly110
Asp113
Asp115
Ser111

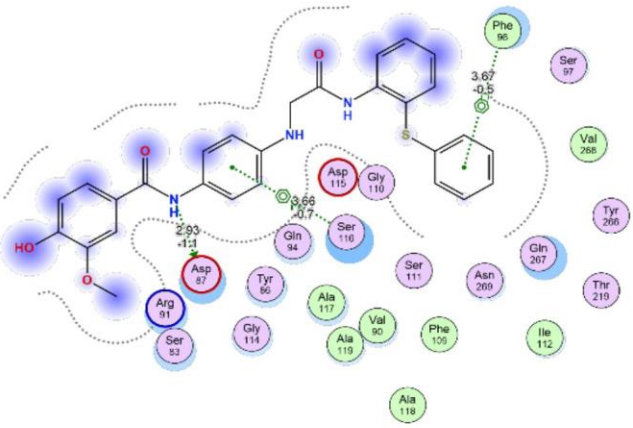
Phe 96
Ser 97
3.67
-0.5
Val 268
NH
Asp 115
Gly 110
3.66
-0.7
Tyr 266
HO
2.93
-1.1
Gln 94
Ser 116
Gln 207
Asp 87
Ser 111
Asn 269
Thr 219
Tyr 86
Arg 91
Ala 117
Val 90
Gly 114
Ser 83
Ala 119
Phe 109
Ile 112
Ala 118

9g

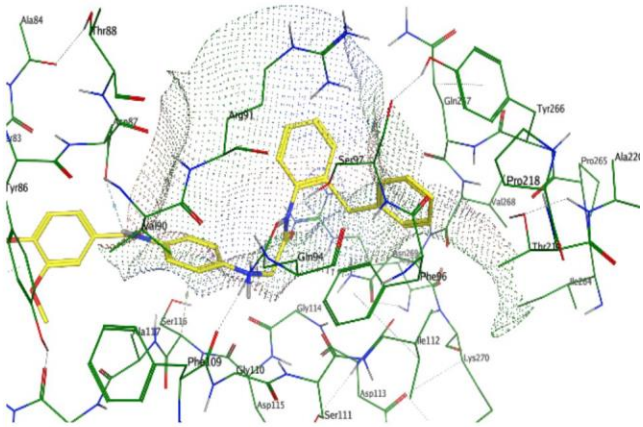
Ala84
Thr88
Arg91
Ser97
Tyr86
Gln267
Tyr266
Pro265
Pro218
Val268
Thr219
Gln94
Phe96
Gly114
Ile112
Lys270
Ser116
Ala117
Phe109
Gly110
Asp113
Asp115
Ser111

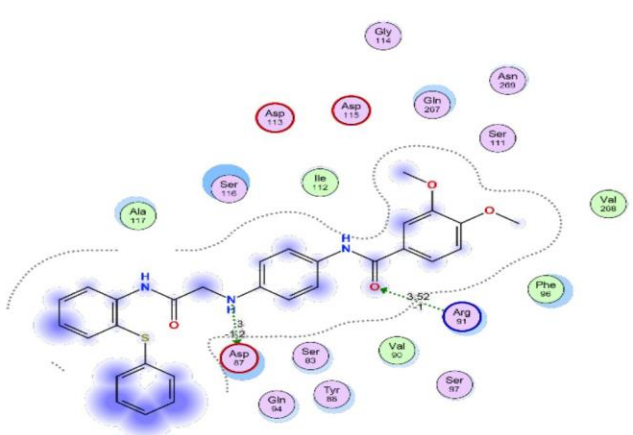
Gly 114
Asn 269
Asp 115
Asp 115
Gln 207
Ser 111
Ser 116
Ile 112
Ala 117
Val 268
H
N
O
O
3.52
-1.1
Phe 96
Arg 91
N
H
3
-1.2
Asp 87
Ser 83
Val 90
Ser 97
Gln 94
Tyr 86

9h

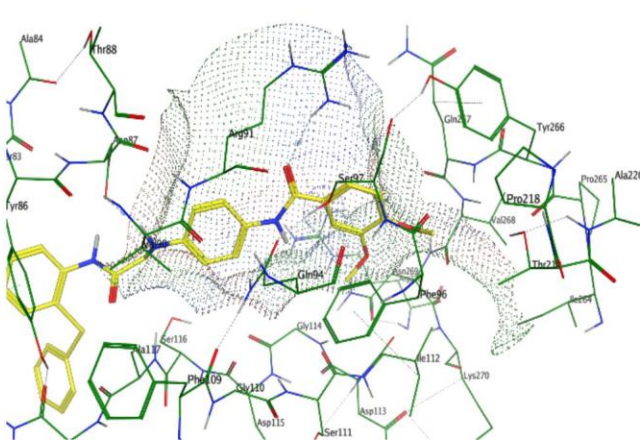
Ala84
Thr88
Arg91
Ser97
Tyr86
Gln267
Tyr266
Pro265
Pro218
Val268
Thr219
Gln94
Phe96
Gly114
Ile112
Lys270
Ser116
Ala117
Phe109
Gly110
Asp113
Asp115
Ser111

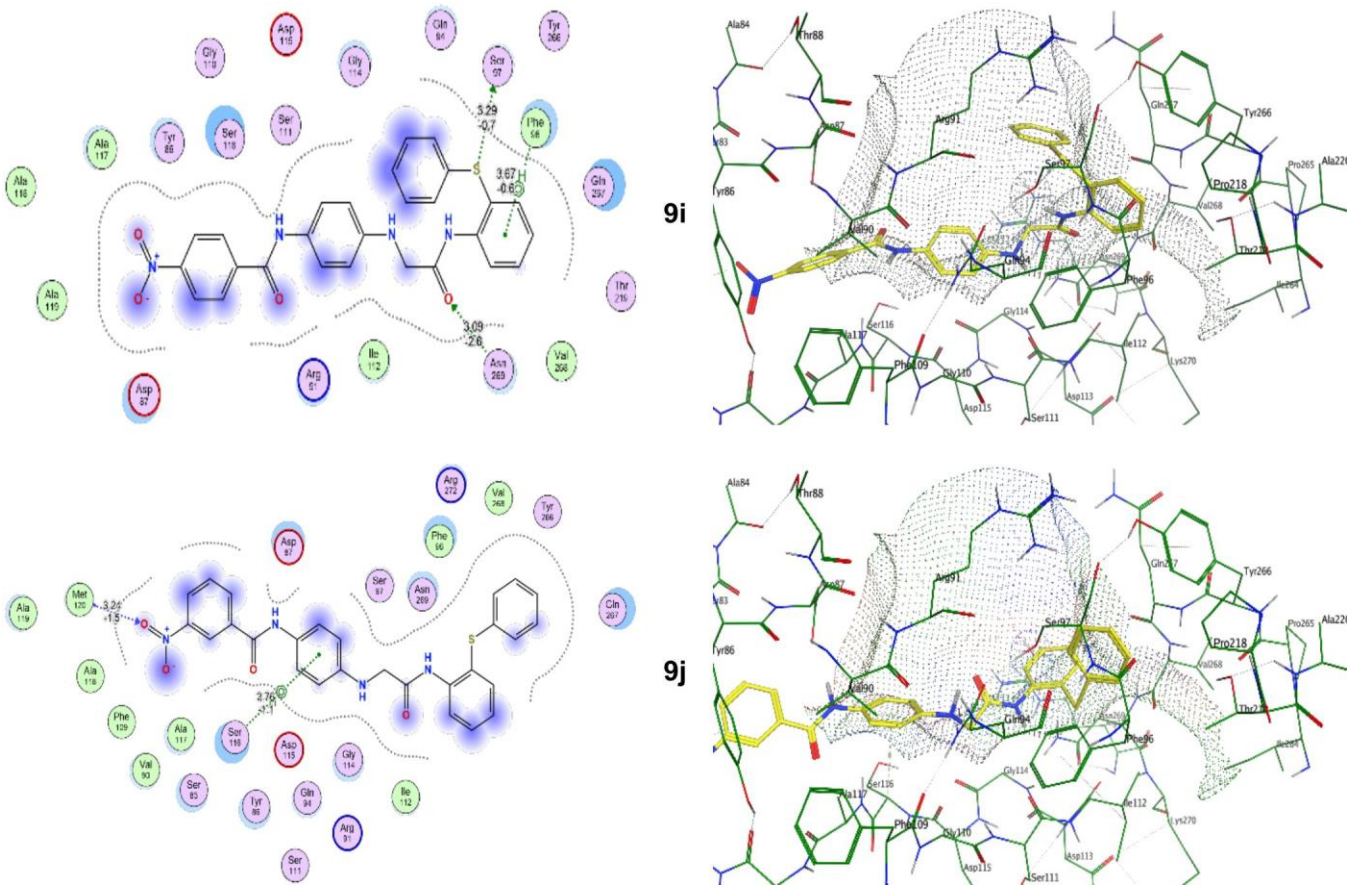

Fig. 1. 2D and 3D binding modes of compounds **9a-j** in the active site of DNA gyrase

groups, favour stronger binding and biological activity. Electron-donating groups like methoxy, when appropriately positioned, also contributed positively. The docking studies aligned well with experimental data, validating the proposed binding interactions with key bacterial residues. These findings demonstrate the promising antibacterial potential of the DAS sulphonamide scaffold, especially compounds **9i**, **9j** and **9b**, as broad-spectrum agents.

ACKNOWLEDGEMENTS

The authors express their gratitude to the Department of Studies in Chemistry, University of Mysore, Manasagangotri, Mysore for providing research laboratory. The authors also express their gratitude to the Department of Chemistry, University of Hyderabad for providing the molecular docking study.

CONFLICT OF INTEREST

The authors declare that there is no conflict of interests regarding the publication of this article.

DECLARATION OF AI-ASSISTED TECHNOLOGIES

During the preparation of this manuscript, the authors used an AI-assisted tool(s) to improve the language. The authors reviewed and edited the content and take full responsibility for the published work.

REFERENCES

1. W.Y. Belay, M. Getachew, B.A. Tegegne, Z.H. Teffera, A. Dagne, T.K. Zeleke, S.A. Wondm, R.B. Abebe, A.A. Gedif, A. Fenta, G. Yirdaw, A. Tilahun and Y. Aschale, *Ther. Adv. Infect. Dis.*, **12**, 20499361251340144 (2025); https://doi.org/10.1177/20499361251340144
2. K. Malarvizhi, D. Ramyadevi, B.N. Vedha Hari, H.B. Sarveswari, A.P. Solomon, H. Fang, R.H. Luo and Y.T. Zheng, *Sci. Rep.*, **13**, 16706 (2023); https://doi.org/10.1038/s41598-023-43103-z
3. C.L. Ventola, *Pharm. Therap.*, **40**, 277 (2015); https://pubmed.ncbi.nlm.nih.gov/25859123/
4. M.E.A. de Kraker, A.J. Stewardson and S. Harbarth, *PLoS Med.*, **13**, e1002184 (2016); https://doi.org/10.1371/journal.pmed.1002184
5. S.F. Koya, S. Ganesh, S. Selvaraj, V.J. Wirtz, S. Galea and P.C. Rockers, *Lancet Reg. Health Southeast Asia*, **4**, 100025 (2022); https://doi.org/10.1016/j.lansea.2022.100025
6. Indian Council of Medical Research. Antimicrobial Resistance Research and Surveillance Network (2021).
7. J. Ranjalkar and S.J. Chandy, *J. Family Med. Prim. Care*, **8**, 1828 (2019); https://doi.org/10.4103/jfmpc.jfmpc_275_19
8. T. Qadir, A. Amin, P.K. Sharma, I. Jeelani and H. Abe, *The Open Med. Chem. J.*, **16**, 1 (2022); https://doi.org/10.2174/18741045-v16-e2202280
9. R.R. Bhandare, C. S.Munikrishnappa, G.V. Suresh Kumar, S.K. Konidala, D.K. Sigalapalli, Y. Vaishnav, S. Chinnam, H. Yasin, A.A. Al-karmalawy and A.B. Shaik, *J. Saudi Chem. Soc.*, **26**, 1 (2022); https://doi.org/10.1016/j.jscs.2022.101447
10. H. Liu, T. Fujiwara, T. Nishikawa, Y. Mishima, H. Nagai, T. Shida, K. Tachibana, H. Kobayashi, R.E. Mangindaan and M. Namikoshi, *Tetrahedron*, **61**, 8611 (2005); https://doi.org/10.1016/j.tet.2005.07.002

11. T. Nakazawa, J. Xu, T. Nishikawa, T. Oda, A. Fujita, K. Ukai, R.E. Mangindaan, H. Rotinsulu, H. Kobayashi and M. Namikoshi, *J. Nat. Prod.*, **70**, 439 (2007); https://doi.org/10.1021/np060593c
12. K.L. Dunbar, D.H. Scharf, A. Litomska and C. Hertweck, *Chem. Rev.*, **117**, 5521 (2017); https://doi.org/10.1021/acs.chemrev.6b00697
13. H. Iino, T. Usui and J. Hanna, *Nat. Commun.*, **6**, 6828 (2015); https://doi.org/10.1038/ncomms7828
14. E. Block, *Angew. Chem. Int. Ed. Engl.*, **31**, 1135 (1992); https://doi.org/10.1002/anie.199211351
15. J.K. Park and S. Lee, *J. Org. Chem.*, **86**, 13790 (2021); https://doi.org/10.1021/acs.joc.1c01657
16. B.P. Chekal, S.M. Guinness, B.M. Lillie, R.W. McLaughlin, C.W. Palmer, R.J. Post, J.E. Sieser, R.A. Singer, G.W. Sluggett, R. Vaidyanathan and G.J. Withbroe, *Org. Process Res. Dev.*, **18**, 266 (2014); https://doi.org/10.1021/op400088k
17. M. Feng, B. Tang, S. H. Liang and X. Jiang, *Curr. Top. Med. Chem.*, **16**, 1200 (2016); https://doi.org/10.2174/1568026615666150915111741
18. K.R. Connolly and M.E. Thase, *Expert Opin. Pharmacother.*, **17**, 421 (2016); https://doi.org/10.1517/14656566.2016.1133588
19. A.M. Fahim, *J. Mol. Struct.*, **1277**, 134871 (2023); https://doi.org/10.1016/j.molstruc.2022.134871
20. A.M. Fahim, *J. Indian Chem. Soc.*, **101**, 101211 (2024); https://doi.org/10.1016/j.jics.2024.101211
21. B.N. Aishwarya, M.S. Chandra, D.M. Manjunath, S. Nanjunda Swamy, V. Katta, U. A. More, B. Ramakrishna, P.S. Yadav and P.B. Shubha, *Rasayan J. Chem.*, **17**, 972 (2024); https://doi.org/10.31788/RJC.2024.1738841
22. K. Sajitha, V.V.P.C. Narayana, V.B. Yesu, D.M. Manjunath, P.S. Yadav, K. Vamsi, D.S. Babu, V. Murali, A.M. Uttam, A. Anitha, J.B. Prasad, M.C. Subhash, D. Srinivasulu and N.V.V. Jyothi, *Asian J. Chem.*, **37**, 166 (2024); https://doi.org/10.14233/ajchem.2025.32973
23. B.Y. Valaparla, Y.R. Kandrakonda, S. Kethineni, V. Katta, S.B. Donka, M.D. Meti, U.A. More, A.G. Damu and S. Doddaga, *Asian J. Chem.*, **37**, 1049 (2025); https://doi.org/10.14233/ajchem.2025.33493
24. E. van Eijk, B. Wittekoek, E.J. Kuijper and W.K. Smits, *J. Antimicrob. Chemother.*, **72**, 1275 (2017); https://doi.org/10.1093/jac/dkw548
25. Y.C. Tse-Dinh, *Infect. Disord. Drug Targets*, **7**, 3 (2007); https://doi.org/10.2174/187152607780090748
26. R.K. Thalji, K. Raha, D. Andreotti, A. Checchia, H. Cui, G. Meneghelli, R. Profeta, F. Tonelli, S. Tommasi, T. Bakshi, B.T. Donovan, A. Howells, S. Jain, C. Nixon, G. Quinque, L. McCloskey, B.D. Bax, M. Neu, P.F. Chan and R.A. Stavenger, *Bioorg. Med. Chem. Lett.*, **29**, 1407 (2019); https://doi.org/10.1016/j.bmcl.2019.03.029
27. T. Khan, K. Sankhe, V. Suvarna, A. Sherje, K. Patel and B. Dravyakar, *Biomed. Pharmacother.*, **103**, 923 (2018); https://doi.org/10.1016/j.biopha.2018.04.021